

Recent QCD and top results at the DØ experiment

B. Tuchming^a

^aCE Saclay, Dapnia/Spp, 91191 Gif-Sur-Yvette, France

The first $p\bar{p}$ data taken at $\sqrt{s}=1.96$ TeV at the DØ experiment have been analyzed. Measurements of jet production rates have been performed and are in agreement with NLO QCD. Evidence for the production of top quarks is also seen in the data. The Run I top mass measurement has been revisited using a method which improves the statistical error.

1. Introduction

The Run II of the $p\bar{p}$ collider Tevatron started in spring 2001. The center of mass energy is 1.96 TeV while it was 1.8 TeV at Run I (1992-1996). The peak luminosity was designed to be $8 \times 10^{31} \text{cm}^{-2} \text{s}^{-1}$, five times higher than at Run I. The integrated luminosity available for physics analysis amounts to about 120pb^{-1} in summer 2003 which is as large as the total luminosity recorded at Run I. Twenty times more data are expected to be accumulated by the end of year 2006. The analysis presented in these proceedings correspond to the first 40pb^{-1} available for physics.

2. The DØ detector

The DØ detector has undergone many upgrades for Run II. To cope with the bunch crossing every 396 ns, 10 times as short as during Run I, and the higher event rates, both read-out and trigger electronics have been replaced. In the inner part of the detector, the tracking system is completely new. It consists of a 2 Tesla solenoid surrounding an eight layer scintillating fiber tracker and a silicon microstrip tracker. To provide discrimination between neutral pions and electrons, a new preshower detector is located between the solenoid and the liquid Argon Uranium sampling calorimeter. The calorimeter which remains essentially unchanged with respect to Run I provides hermetic coverage of the interactions and a good resolution. The

outer part of the detector is a muon spectrometer consisting of three layers of proportional drift tube chambers, scintillation counters and a 1.5 Tesla iron toroid.

A forward proton detector has been commissioned for Run II. It consists of nine momentum spectrometers made of 6 Roman Pots. They are located at 23, 33, 57 and 59 down the beam from the interaction point. By tagging the proton deflected at low angle, these detectors are dedicated to the measurement of single diffractive and double diffractive processes and will allow to probe the pomeron structure functions. A first version of alignment of the Roman pots has been performed in spring 2003 and the detector is now ready to begin its physics program.

3. Measurements of jet production

Jet physics at the Tevatron Run II is a unique opportunity to test next-to-leading order QCD (NLO) at new energies with a large statistics. The proton structure can be probed at large x , especially the gluon parton density function (PDF). At $\sqrt{s} = 1.96$ TeV, the production of jets is enhanced by roughly a factor two for transverse energy larger than 400 GeV compared to Run I as can be seen in figure 1. New physics might also be discovered: quark compositeness would show up as an enhancement in the production at high transverse energy while new gauge bosons would be seen as a resonance in the dijet mass spectrum with increased sensitivity to higher masses.

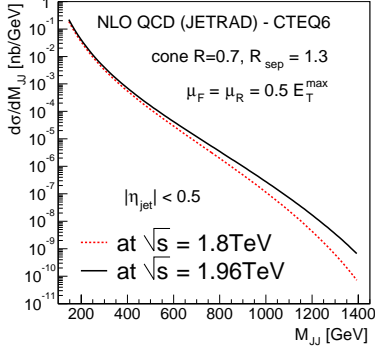


Figure 1. NLO prediction for the production of dijet at the energy of Run I and Run II.

3.1. Jet reconstruction

Jets are built using an iterative cone algorithm with radius $R = \sqrt{\Delta\eta^2 + \Delta\phi^2} = 0.7$ [1]. A new feature compared to Run I is a two pass algorithm. In the second pass, the midpoints between two jets are used as new seed. The jets are also built using four vectors instead of scalar quantities.

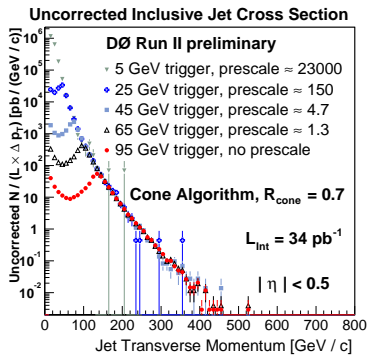


Figure 2. Uncorrected cross section for the production of jets as a function of their transverse momentum for different triggers and prescales.

The quality criteria to reduce the background and ensure that an event has properly been reconstructed are as follows. The vertex of the event has to be reconstructed with five charged tracks. The coordinate along the beam of this vertex is required to be within ± 50 cm. The ratio between the missing transverse energy and the p_T of the leading jet should be lower than 0.7. The jets are required to be central, in the region $|\eta| < 0.5$. Some cuts on the shower shape are also performed to reduced the fake rate due to calorimeter background.

The data for the jet measurement corresponds to an integrated luminosity of about 34 pb^{-1} and was collected using six jet triggers. Each of them requires a localized energy deposited in the calorimeter and a reconstructed jet transverse energy threshold of respectively 5, 25, 45, 65, 95 and 125 GeV. Figure 2 shows the uncorrected cross sections for the production of jets using these triggers, with a perfect overlap between two adjacent triggers when being sufficiently far from the threshold. The unfolding of the energy resolution is not done at this level.

3.2. Energy correction and resolution

Giving the stiff dependence of the jet production rate with the jet energy, it is crucial to correct the data for any bias in the jet energy determination and unfold the resolution effect.

The corrected jet energy is given by $E_{corr} = \frac{E_{uncorr} - O}{R \cdot S}$, where O is the offset due to noise, pile-up and underlying events, S is the fraction of energy leaking out of the cone due to showering and R is the calorimeter response, different from one due to non-linearity, dead material and different response for γ/π^0 and π^\pm .

This response, shown in figure 3, is determined using γ +jet events where the photon transverse energy is expected to balance the jet energy. Because of the limited statistics of high energy γ +jet events, some extrapolation has to be performed and the uncertainty on the jet energy scale is quite substantial. This is the main source of systematics for the following cross sections measurements. This is expected to be dramatically improved in the near future, when more data will be accumulated in DØ.

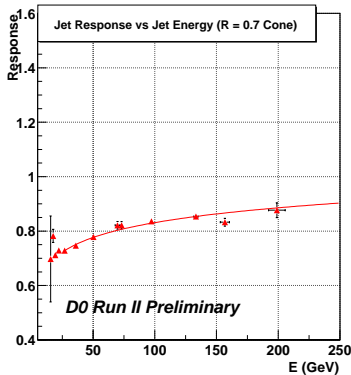


Figure 3. Jet energy response as a function of the jet energy.

The jet momentum resolution is measured using back to back dijet events. The asymmetry $A = \frac{p_T^{jet1} - p_T^{jet2}}{p_T^{jet1} + p_T^{jet2}}$ gives the relative resolution in a straightforward way: $\frac{\sigma_{p_T}}{p_T} = \sqrt{2}\sigma_A$. This resolution is displayed in figure 4.

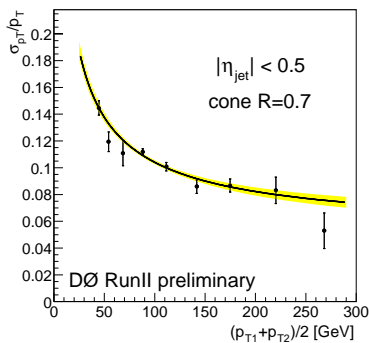


Figure 4. Jet momentum resolution as a function of the two jet transverse momenta.

3.3. Inclusive jet cross section

The inclusive cross section of jet production as a function of the momentum is given by

$\frac{d\sigma}{dp_T} = \frac{N_{jet}}{L\Delta p_T} \times \frac{C_{unsmear}}{\epsilon}$, where C is the unsmearing factor accounting for resolution effects and ϵ is the selection efficiency determined with the data. The cross section, which falls by six orders of magnitude between $p_T=50$ GeV/c and $p_T=500$ GeV/c is shown in figure 5. The 10% uncertainty on the luminosity which is bin-to-bin correlated is not taken into account in this plot.

The cross section is compared to the results of NLO QCD calculations made with the JETRAD[2] Monte Carlo generator using the CTEQ6M[3] and MRST2001[4] PDF in figure 5. Within the errors, which are mainly due to the uncertainty on the energy scale, the data are in agreement with the NLO prediction.

3.4. Dijet cross section

The dijet cross section is measured by counting the events with at least two jets in the central region $|\eta| < 0.5$ and unfolding the resolution effects. The cross section as a function of the dijet mass is shown in figure 6. The 10% uncertainty on the luminosity is not taken into account in this plot. These results agree within the error with the QCD NLO prediction as shown in figure 6.

4. Top production at Run II

4.1. Top quark at DØ

The discovery of the top quark occurred at Tevatron Run I in 1994 [5,6]. The production cross section of top pairs was measured to be around 6 pb and the top mass was measured at DØ with an accuracy of 8 GeV/c² [8].

At Run II, thanks to the higher center of mass energy, the production of top pairs is enhanced by 30%. With a few inverse femtobarn, many topics of top physics should be covered: measurement of the production cross section, measurement of the mass with an accuracy of 2 or 3 GeV/c², spin and polarization studies, branching ratio determination, W helicity measurement, search for non Standard Model decays, and electroweak production of single top.

At this earlier stage of the Run II data taking, the main goal is the “rediscovery” of the top quark. The analysis presented in the following

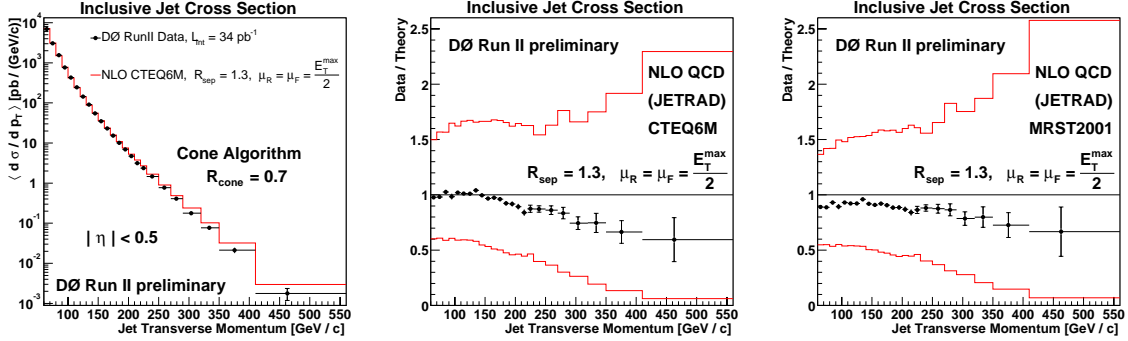


Figure 5. Inclusive jet cross section as a function of the jet transverse momentum and comparison to NLO QCD using the CTEQ6M and the MRST2001 PDF.

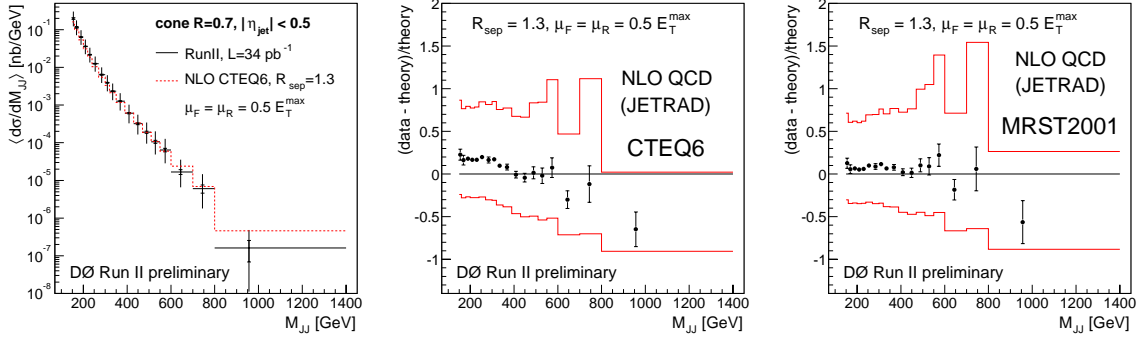


Figure 6. Dijet cross section as a function of the dijet mass and comparison to NLO QCD using the CTEQ6M and the MRST2001 PDF.

correspond to about 50 pb^{-1} collected before January 2003.

4.2. Top quark final states

The top quark decays into a W boson and a b quark. According to the W branching ratio, one can distinguish two sorts of signatures of top pair production.

1. the dilepton+jets where both W 's decay into lepton+neutrino are classified as di-electron+2 jets, di-muon+2 jets and electron-muon+2 jets. These events are

characterized by the presence of two high p_T isolated muons or electrons, two high p_T jets and a large missing transverse energy.

2. lepton+jets where one of the W 's decays hadronically. We look for events with one high p_T isolated muon or electron, a large missing transverse energy and at least four jets.

All these channels may benefit from b -tagging techniques thanks to the presence of two b -quarks in the final state: secondary vertex tag, impact parameter tag and soft lepton tag. Currently,

only soft muon tag has been used in the lepton+jets channels.

4.3. Dilepton channels

Events are selected by demanding two leptons with $p_T > 15$ GeV/c. This cut is raised to 20 GeV/c in the ee channel. The muons have to be isolated from calorimeter deposits and high p_T tracks. The missing transverse energy fullfills $E_T > 25$ GeV. In addition, when the dilepton mass is close to the Z mass ($70 < M_{\mu\mu} < 110$ GeV/c² in $\mu\mu$ channel, $75 < M_{ee} < 105$ GeV/c² in the ee channel) the cut is raised to $\cancel{E}_T > 40$ GeV. Two reconstructed jets with transverse energy higher than 20 GeV and in the region $|\eta| < 2.5$ are also required. The scalar transverse energy $H_T = \sum_{jets, leptons} E_T$, has to be higher than 120 GeV. This cut is lowered to 100 GeV in the $\mu\mu$ channel.

The background consists of WW production, WZ production, Z production and QCD (mainly heavy flavour) events. It can be separated in two parts: the instrumental background and the physical background. The instrumental background is estimated from the data and consists of either transverse energy mismeasurement or jets faking electrons or muons from heavy flavours being seen as isolated from their parent jets. The physical background, has the same signature as the signal (eg: $Z \rightarrow \tau\tau$) and is estimated with the help of Monte Carlo simulations. The results of the selections are quoted in table 1.

4.4. Lepton plus jets channels

The events are preselected by demanding that the lepton p_T and the missing transverse energy be higher than 20 GeV. Four jets with $p_T > 15$ GeV/c in the region $|\eta| < 2.5$ are required. The muon and the electron have to be isolated.

The background for this channels is made of W +jets events, QCD events where a jet fakes an electron, or isolated muons produced within heavy flavour events. The fake rate of electron identification or isolated muons is extracted from the data. It is then used to subtract the QCD and heavy flavour background and determine the rate of W +jets events as a function of the number of jets (see figure 7).

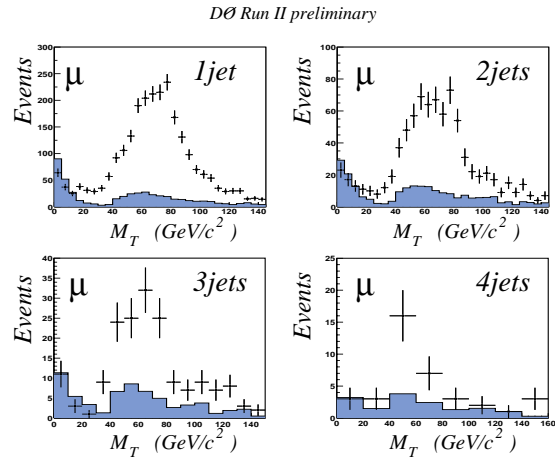


Figure 7. Transverse mass for μ +jets events. The colored histograms are the estimated contribution from the QCD background.

This rate follows the Berends empirical scaling law $\frac{\sigma(W+(n+1)jets)}{\sigma(W+njets)} = \alpha$ as shown in figure 8. This law allows to extrapolate the contribution of W +jets events to the leptons+4 jets candidates. Then topological cuts are applied on the scalar transverse energy and the applanarity of the events to get rid of the remaining background. The results of these selections are shown in table 1.

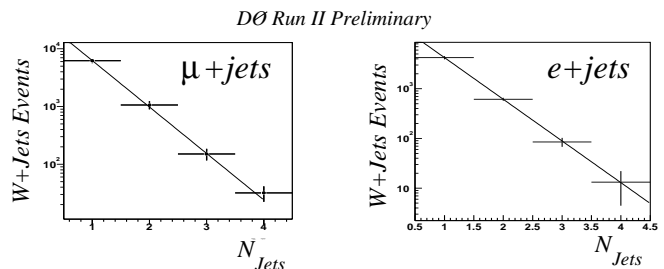


Figure 8. Production rate of W +jets events as a function of the number of jets.

	$e\mu$ 33 pb ⁻¹	$\mu\mu$ 42 pb ⁻¹	ee 48 pb ⁻¹
$Z \rightarrow \tau\tau \rightarrow \ell\ell$.02 ± .01	.02 ± .02	.02 ± .02
$WW \rightarrow \ell\ell$.001 ± .001	.00 ± .00	.001 ± .001
$Z \rightarrow \ell\ell$	–	.20 ± .12	
Drell Yan → $\ell\ell$	–	.20 ± .12	.98 ± .48
QCD, W +jets	.05 ± .01	.18 ± .18	
All background	.07 ± .01	.60 ± .30	1.0 ± .48
Expected signal	.50 ± .01	.30 ± .04	.25 ± .02
Observed	1	2	4

	e +jets 40 pb ⁻¹	μ +jets 49.5 pb ⁻¹	μ +jets/ μ 40 pb ⁻¹	e +jets/ μ 49.5 pb ⁻¹
All background	2.7 ± 1.1	2.7 ± .6	.7 ± .4	.2 ± .1
Expected signal	2.4	1.8	.8	.5
Observed	4	4	0	2

Table 1
Signal and background expectations and observed events for the different top quark channels.

4.5. Lepton plus jets plus soft muon tag

In addition of a high p_T lepton, the presence of a soft muon of transverse momentum higher than 4 GeV/ c is demanded. For the signal, it is supposed to be produced in the decay of a b-quark so it is required to be within $\Delta R < 0.5$ of the jet axis. As the presence of this soft muon is a very stringent requirement, the selection is basically the same as in the previous section but the cuts are loosend and only three recontructed jets are required. The analysis ends up with a few selected top candidate events as shown in table 1.

4.6. top production summary

The results of the different channels quoted in the table 1 are combined to compute the cross section for the top pair production at $\sqrt{s} = 1.96$ TeV:

$$\sigma_{t\bar{t}} = 8.5_{-3.6}^{+4.5} \text{ (stat)} \text{ }_{-3.5}^{+6.3} \text{ (sys)} \pm 0.8 \text{ (lumi)} \text{ pb}$$

The contribution of the different channels are shown in figure 9.

This result is expected to be greatly improved in the near future tanks to the increase of luminosity, a better tracking efficiency and resolution and the usage of secondary vertex based tagging of b-quarks.

5. Top mass measurement with Run I data

Within the Standard Model, the top quark mass, along with the mass of the W boson, is a key parameter to determine the mass of the Higgs boson through radiative correction. Combined with all other electroweak observables, it provides a powerfull probe to test the consistency of the Standard Model and search for new physics. The best value of the top quark mass has been obtained by combining all channels of the DØ and CDF mass measurement at Tevatron Run I[7]:

$$m_{top} = 174.4 \pm 5.1 \text{ GeV}/c^2$$

5.1. DØ Run I analysis

The measurement of the top mass using Run I data, in the lepton+jets channels, is described in [8]. After applying the selection cuts, 91 $t\bar{t}$ candidate events are selected. The two-dimensional probability density function of the fitted top mass and a multivariate discriminant is built for these events. This allows to compute a likelihood function. The maximization of the likelihood yields the result:

$$m_{top} = 173.3 \pm 5.6 \text{ (stat)} \pm 5.3 \text{ (sys)} \text{ GeV}/c^2$$

5.2. Reanalysis of the data

The same selection and the same data set ($\mathcal{L} = 125 \text{ pb}^{-1}$) as in [8] is used. Some tighter criteria

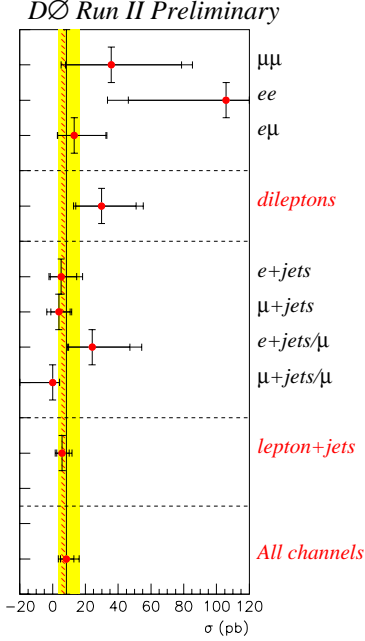


Figure 9. cross section results summary, including the contributions from the different channels

are added to get a purer $t\bar{t}$ sample. Only events with exactly four jets are selected so that a one-to-one matching between partons and jets can be assumed. The probability of $t\bar{t}$ production is computed for each event taking into account the full kinematics. It reads:

$$P_{t\bar{t}}(x) = \frac{1}{12\sigma_{t\bar{t}}} \int d\rho_1 dm_1^2 dM_1^2 dm_2^2 dM_2^2 \times \sum_{perm,\nu} |\mathcal{M}|^2 \frac{f(q_1)f(q_2)}{|q_1||q_2|} \Phi_6 W(x, y),$$

where the sum is over all 12 permutations of the jets and all possible values of ν z-momenta, \mathcal{M} is the LO matrix element for the process, $f(q_{1,2})$ are the PDF's for the incident partons, Φ_6 is the phase space factor for the 6-object final state and the $W(x, y)$ correspond to the mapping between real (y) and measured momenta (x), accounting for resolution effects. The integration variables

are the top masses, $m_{1,2}$, the W masses, $M_{1,2}$, and the energy of the u-type jet of the hadronic W -decay, ρ_1 . The background probability P_{bkg} is also computed with the help of VECBOS[9]. The likelihood for the $N = 22$ candidate events remaining after the selection reads:

$$-\log \mathcal{L}(m_t) = -\sum_{i=1}^N \log(c_1 P_{t\bar{t}}(x_i, m_t) + c_2 P_{bkg}(x_i)) + N \int A(x) (\log(c_1 P_{t\bar{t}}(x, m_t) + c_2 P_{bkg}(x))) dx,$$

where $A(x)$ is the acceptance function and c_1 and c_2 are the relative proportions of signal and background. By minimizing this expression with respect to the mass hypothesis m_t , as shown in figure 10, one obtains the best value of the top mass, m_t and the c_1 and c_2 parameters. The preliminary result is:

$$m_{top} = 180.1 \pm 3.6(\text{stat}) \pm 4.0(\text{sys}) \text{ GeV}/c^2$$

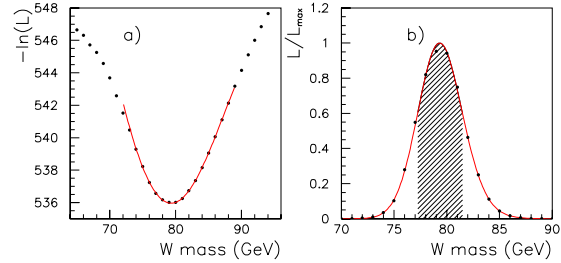


Figure 10. Likelihood function used to determine the top mass.

It must be noticed that resolution effects are taken into account on an event by event basis in the $W(x, y)$ term, whereas in the previous method [8], the average resolutions were actually considered. Therefore poorly measured events are deweighted while sharply measured events contribute more to the final results. This explains why the statistical uncertainty has been reduced while using only a subset of the event

sample. The main contributions to the systematic uncertainty come from the jet energy scale (3.6 GeV/c²), the modeling of the $t\bar{t}$ production (1.5 GeV/c²), the modeling of background (1.0 GeV/c²), the noise and multiple interactions (1.3 GeV/c²), the PDF uncertainty (0.2 GeV/c²).

6. Conclusion

DØ has started its QCD physics program by measuring the inclusive jet and dijet cross sections. The cross sections are in good agreement with the prediction of NLO QCD. In the near future the accuracy of these results is expected to be improved thanks to a larger amount of data, a better understanding of the jet energy scale and an extended rapidity coverage.

DØ has also established the presence of top quark events in its data, which is the preliminary step to the Run II top quark physics program.

Using Run I data, a new top quark mass measurement has been performed leading to a substantial reduction in the uncertainty. This measurement reaches the level of accuracy of the previous combined DØ and CDF result.

REFERENCES

1. G. Blazey, et al., Proc. of Physics at Run II: QCD and Weak Boson Physics Workshop, Batavia, IL (Nov. 4-6, 1999), FERMILAB-CONF-00-092-E.
2. W. T. Giele, E. W. Glover and D. A. Kosower, “*Higher Order Corrections To Jet Cross-Sections In Hadron Colliders*,” Nucl. Phys. B **403**, 633 (1993)
3. J. Pumplin, D. R. Stump, J. Huston, H. L. Lai, P. Nadolsky and W. K. Tung, “*New generation of parton distributions with uncertainties from global QCD analysis*,” JHEP **0207**, 012 (2002)
4. A. D. Martin, R. G. Roberts, W. J. Stirling and R. S. Thorne, “*MRST2001: Partons and alpha(s) from precise deep inelastic scattering and Tevatron jet data*,” Eur. Phys. J. C **23**, 73 (2002)
5. S. Abachi et al. [DØ Collaboration], “*Observation of the top quark*,” Phys. Rev. Lett. **74**, 2632 (1995)
6. F. Abe et al. [CDF Collaboration], “*Observation of top quark production in anti-p p collisions*,” Phys. Rev. Lett. **74**, 2626 (1995)
7. Particle Data Group. <http://pdg.lbl.gov> (2002)
8. B. Abbott et al. [DØ Collaboration], “*Direct measurement of the top quark mass at DØ*,” Phys. Rev. D **58**, 052001 (1998)
9. F. A. Berends, H. Kuijff, B. Tausk and W. T. Giele, “*On The Production Of A W And Jets At Hadron Colliders*,” Nucl. Phys. B **357**, 32 (1991).